Effect of Cable Stiffness and Waves Parameters on the Dynamic Responses of Submerged Floating Tunnel

Naik Muhammad, Azmatullah Khan, Zafar Baloch, Muhammad Habib, Saeedullah Jan Mandokhail

Department of Civil Engineering, Faculty of Engineering and Architecture, Balochistan University of Information Technology, Engineering and Management Sciences, Quetta, Pakistan

Abstract

Submerged floating tunnel (SFT) is a new structural solution for waterway crossings compared to the classical solutions such as cable supported bridge, immersed tunnel or underground tunnel. An SFT is subjected to extreme waves, currents, earthquakes and other environmental loadings. The effect of key structural and waves parameters are important from the design perspective for an SFT. This study, the dynamic responses of SFT are evaluated using truss and catenary cables to check the effect of cable stiffness. The second part of this study deals with the effect of wave height and wave period on the dynamic responses of SFT. 3D truss and 3D catenary cables give very similar dynamic responses under waves and vertical ground motions. The wave height and wave period mainly control the dynamic behavior of SFT.

Key words: Submerged Floating Tunnel; Truss Cable; Catenary Cable; Effect of Waves Parameters

Corresponding author's email: naik_babar2954@yahoo.com

INTRODUCTION

For shallow and narrow waterway crossing, it is easy to cross by constructing cable-supported bridge, immersed tunnel or underground tunnel but it becomes difficult and uneconomical for wide and deep straits. In addition, the construction cost increases for the conventional structures when the width of waterway crossing goes on increasing. SFT is a watertight structure, the balance between pre-tension in the mooring cables and net positive buoyancy (or residual buoyancy) maintains the structural stability of SFT. Because the cost of an SFT per unit length remains almost constant with increasing length (Ahrens, 1997; Faggiano et al., 2005), so it is an economical alternative for waterway crossings in comparison to long span suspension bridges, underground tunnels or immersed tunnels, especially for deep and wide crossings. In addition, an SFT is more advantages such as it is not limited to some specific geographic terrain and does not interfere with water surface vessels. The research developments regarding the response of SFT under hydrodynamic waves and current, seismic loadings are presented for last three decades. The fundamental aspects of the dynamic behavior of an SFT under seismic and sea waves effects was presented by (Brancaleoni et al., 1989). The local problem of fluid-structure interaction (FSI) of the SFT using two-dimensional model was made by (Okstad et al., 1998), later on, a more comprehensive presentation of FSI was made by (Remseth et al., 1999) using finite element implementation of the Naiver-Stokes equation. The dynamic response of SFT under hydrodynamic waves and seismic excitations have been studied by many researchers using simplified numerical models (Di Pilato et al., 2008; Fogazzi et al., 2000), however, in these studies more attention is devoted to the design solution encompassing slender bars as anchor/mooring elements. The vortex-induced vibrations of mooring/anchor cables caused by water currents is discussed by (Li et al., 2006; Luoa et al., 2015; Yiqiang et al., 2012). The important design parameters such as length of tunnel, buoyancy to weight ratio, spacing of anchoring/mooring cables, inclination of the mooring cable with horizontal, depth of submergence need to properly investigate for the realization of SFT. However, limited studies are available focusing the design of parameters of SFT. The effect of tunnel length, structural damping and buoyancy to weight ratio on the response of SFT was studied by (Long et al., 2015; Long et al., 2009) using finite element models of the SFT through commercial software. However, the effect of cable stiffness and waves parameters are not studied well and need to be investigated in more details. The study evaluates the dynamic responses of SFT to check the effect of cable stiffness and waves parameters including wave height and wave period. Some important conclusions are given based on the numerical simulations performed in this study.

MATERIALS AND METHODS

Modeling of waves and currents

The ocean waves and currents are modeled by well-known Airy wave theory, and the wave forces are calculated from the modified Morison's equation, which is given as (Chakrabarti, 1987; Muhammad et al., 2017; Muhammad et al., 2017):

$$\{f(q,t)\} = \frac{1}{2} C_D \rho_w D \{|\dot{w}_\perp \pm U - \dot{q}_\perp|(\dot{w}_\perp \pm U - \dot{q}_\perp)\} + C_M \rho_w \frac{\pi D^2}{4}\{\ddot{w}_\perp\} - C_A \rho_w \frac{\pi D^2}{4}\{\ddot{q}_\perp\} \tag{1}$$

where subscript denotes the perpendicular components with respect to element axis. ρ_w is the density of water, D is the external diameter of SFT, C_D is the drag coefficient, C_M is the inertia coefficient, $C_A = C_M - 1$ is the added mass coefficient, and are water particle velocity and acceleration, while and are structural velocity and acceleration respectively. U is the velocity of water currents acting at the centerline of SFT.

Governing equations of motion

The equations of motion for the SFT subjected to waves and multi-support seismic excitations can be written as (Muhammad, 2018):

$$\begin{bmatrix} [M] & [M_g] \\ [M_g]^T & [M_{gg}] \end{bmatrix} \begin{Bmatrix} \{q_{sr}\} \\ \{q_g\} \end{Bmatrix} + \begin{bmatrix} [C] & [C_g] \\ [C_g]^T & [C_{gg}] \end{bmatrix} \begin{Bmatrix} \{q_{sr}\} \\ \{q_g\} \end{Bmatrix} + \begin{bmatrix} [K] & [K_g] \\ [K_g]^T & [K_{gg}] \end{bmatrix} \begin{Bmatrix} \{q_{sr}\} \\ \{q_g\} \end{Bmatrix} = \begin{Bmatrix} \{f(t)\} \\ \{p_{eff}(t)\} \end{Bmatrix} \tag{2}$$

where the subscript *sr* represents the unrestrained degrees of freedom (DOFs) in the system including both tunnel and cables DOFs, and *g* represents the support DOFs. $\{f(t)\}$ is time-dependent wave (hydrodynamic) forces. The $p_{eff}(t)$ is the effective seismic forces at the supports and is given as:

$$\{p_{eff}\}_{N\times1} = -[M][i]\{u_g\} \tag{3}$$

where $[i]$ is the influence matrix; $\{u_g\}$ is the seismic ground motion acceleration vector acting at the supports.

The matrices $[M]$, $[K]$, and $[C]$ are given as

$$[M] = [[M_t] + [M_c] + [M_{at}] + [M_{ac}]] \tag{4}$$

$$[K] = [K_e] + [K_c] \tag{5}$$

$$[C] = \beta_1[[K_e] + [K_c]] + \beta_2[[M_t] + [M_c] + [M_{at}] + [M_{ac}]] \tag{6}$$

where $[M_t]$ is the mass matrix of the tunnel; $[M_{at}]$, $[M_{ac}]$ are the added mass matrices for the tunnel and cables, respectively ; $[M_c]$ is the mass matrix of the cables; $[K_e]$ is the elastic stiffness of the tunnel calculated from 3D beam element; $[K_c]$ is the nonlinear mooring cable stiffness calculated by catenary element; β_1 and β_2 are the Rayleigh damping coefficients; ζ is the modal damping ratio; ω_i , ω_j are the i^{th} and j^{th} modal natural frequencies of the structure, respectively. For obtaining the damping matrix, 2.5% modal damping ratio was used (Veritas, 2006).

The displacement $\{q\}$ vector is given as

$$\{q\} = \{\{q_t\} + \{q_c\}\} \quad (7)$$

where $\{q_t\}$ is tunnel displacements and $\{q_c\}$ is mooring cable displacements and these matrices for one element is given as

$$\{q_t\} = [q_{X1} \; q_{Y1} \; q_{Z1} \; \theta_{X1} \; \theta_{Y1} \; \theta_{Z1} \; q_{X2} \; q_{Y2} \; q_{Z2} \; \theta_{X2} \; \theta_{Y2} \; \theta_{Z2}]^T \quad (8)$$

$$\{q_c\} = \{q_{X1} \quad q_{Y1} \quad q_{Z1} \quad q_{X2} \quad q_{Y2} \quad q_{Z2}\}^T \quad (9)$$

In the present paper, the tunnel was modeled by 50 3D beam elements, and each cable was modeled by 5 catenary elements.
The solution of the nonlinear equations of motion (Equation 2) is calculated using the Newmark average acceleration method for time integration and the modified Newton-Raphson method for the equilibrium correction at each time step.

Numerical example

An SFT model to be built in Qindao Lake, China is taken as an example in this paper. The input parameters are based on the environmental conditions of Qindao Lake China and described by (Muhammad et al., 2017) unless mentioned otherwise. The SFT model used here is made somehow more symmetric, and all cables have an inclination of 45º. The SFT model used for numerical simulations is shown in Figure 1. The notation C1, to C6, represent the cable's numbering from 1 to 6, respectively. The pretensions in the cables are calculated from the net buoyancy acting on the tunnel and given in (Muhammad, 2018).

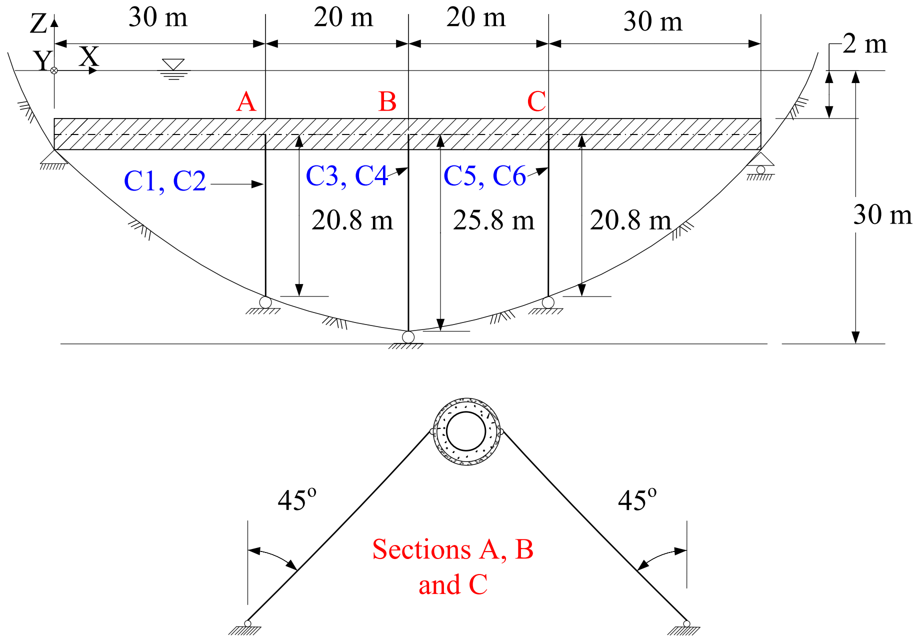

Figure 1: Structural model of SFT used for numerical simulations

RESULTS AND DISCUSSION

Comparison of dynamic responses using 3D truss and 3D catenary

In this section a comparison of the SFT responses and cable top tension is presented using two type of cable elements: (1) 3D catenary element: this element is based on the procedure described in reference (Muhammad et al., 2018) . This element incorporate the geometric nonlinear analysis considering only self-weight of the cable element. (2) 3D truss element: this element is based on a 3D space truss considering both elastic and geometric stiffness, and implemented in the geometric nonlinear procedure. The ground motions are modeled by the procedure outlined in (Muhammad, 2018). Comparison of the SFT displacements and cable top tensions, using truss and catenary cables at the location B under waves and vertical ground motions, is shown in Figure 2. The SFT vibrates with large amplitude displacements under these conditions. The SFT maximum horizontal displacements are 0.021 m and 0.021 m, using truss and catenary, respectively. Similarly, The SFT maximum vertical displacements are 0.026 m and 0.026 m, using truss and catenary cables, respectively. The maxim cable top tensions in the cable 3 (C3) are 0.734×10^6 N, and 0.734×10^6 N, using truss and catenary cables, respectively. Similarly, the maxim cable top tensions in the cable 4 (C4) are 0.784×10^6 N, and 0.784×10^6 N, using truss and catenary cables, respectively. There is a relative difference between truss and catenary cables of 0.00 % SFT horizontal displacements, 0.01 % SFT vertical displacements, 0.02 % cable 3 top tensions, and 0.02 % cable 4 top tensions, respectively. The difference in the responses using centenary and truss cables is small in the present analysis case, however catenary cable gives slightly larger responses and this element could be very useful for very deep SFT problems, having very long cables. Comparison of the SFT maximum positive displacements and bending moments envelope curves using truss and catenary cables under waves and vertical ground motions, are shown in Figure 3. The SFT horizontal displacements (q_Y), the SFT vertical displacements (q_Z), the SFT horizontal bending moments (M_Z), and the SFT vertical bending moments (M_Y) are very similar, using truss and catenary cables. The shape of the bending moments give clear understanding of the cable stiffness.

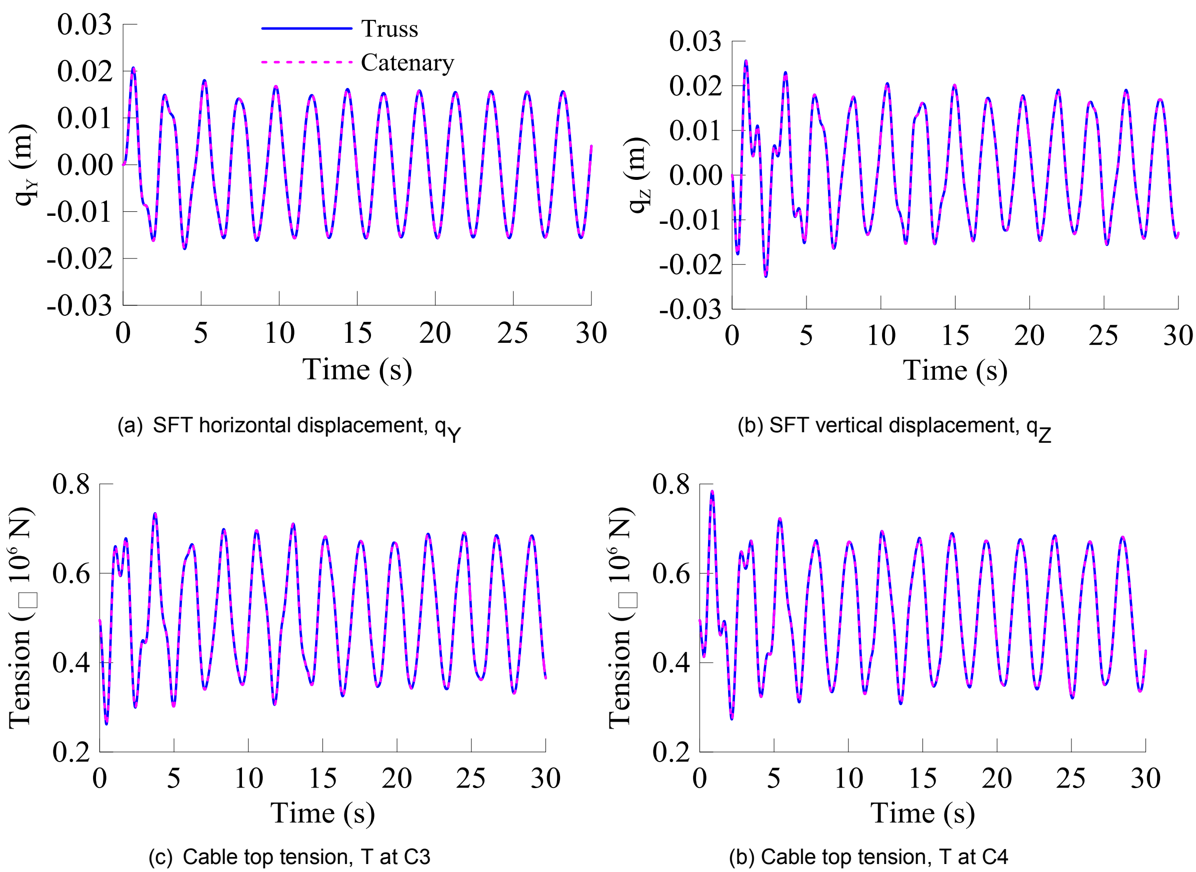

(a) SFT horizontal displacement, q_Y

(b) SFT vertical displacement, q_Z

(c) Cable top tension, T at C3

(b) Cable top tension, T at C4

Figure 2: Comparison of the SFT displacements and cable top tensions, using truss and catenary cables at the location B under waves and vertical ground motions (H=1 m, T=2.3 s, ζ=2.5%)

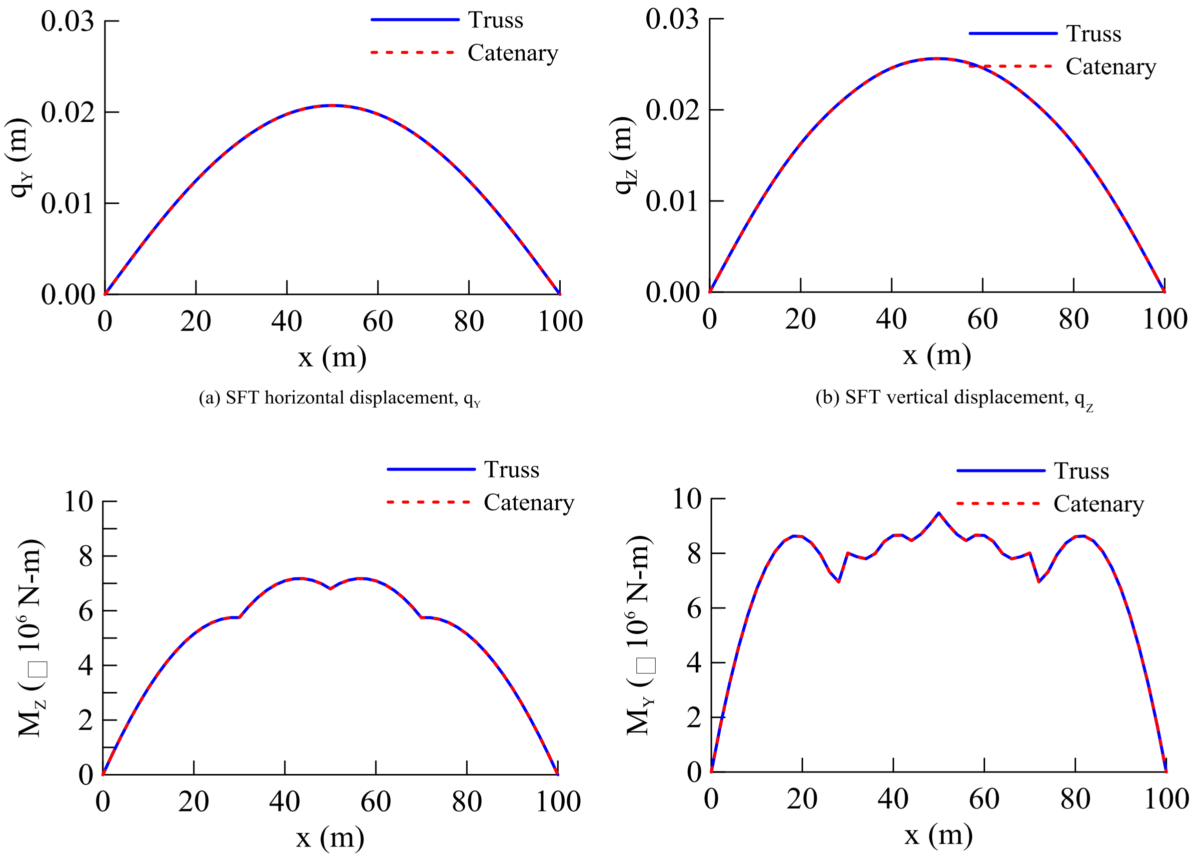

(a) SFT horizontal displacement, q_Y

(b) SFT vertical displacement, q_Z

(c) SFT horizontal bending moment, M_Z

(d) SFT vertical bending moment, M_Y

Figure 3: Comparison of the SFT maximum positive displacements and bending moments envelope curves using truss and catenary cables under waves and vertical ground motions (H=1 m, T=2.3, ζ=2.5%)

Effect of wave height and wave period on dynamic response of SFT

The waves are dominant actions in the dynamic analysis of SFT. Therefore, it is important to study the effect of important waves parameters on the responses of SFT. In this section, the effect of wave height (H) and wave period (T) on the responses of SFT is evaluated in more details. Effect of wave height (H) on maximum SFT responses and maximum cable top tensions at location B under waves is shown in Fig. 4. The cable horizontal displacements (q_Y) and vertical displacements (q_Z) increase linearly with increase of wave height. Similarly, the cable top tension increase with wave height. The wave height greater than 2 m cause the mooring cables to have slack conditions, and the top tension falls well below the initial pretension (0.5×10^6 N) in the cable. In the present study, the nominal tension of the cables having diameter of 0.06 m is 3.14×10^6 N. There is no tension that cross the nominal tension level of the used mooring cables.

Effect of wave period (T) on the maximum SFT responses and maximum cable top tensions at location B under waves is shown in Fig. 5. The SFT horizontal displacements (q_Y) and vertical displacements (q_Z) increase with T. Similarly, the cable top tension increase slightly with T. The SFT displacements have a kind of parabolic increment with the wave period. The cable maximum top tension increase with the wave period, while the minimum tensions decrees with increase of wave period.

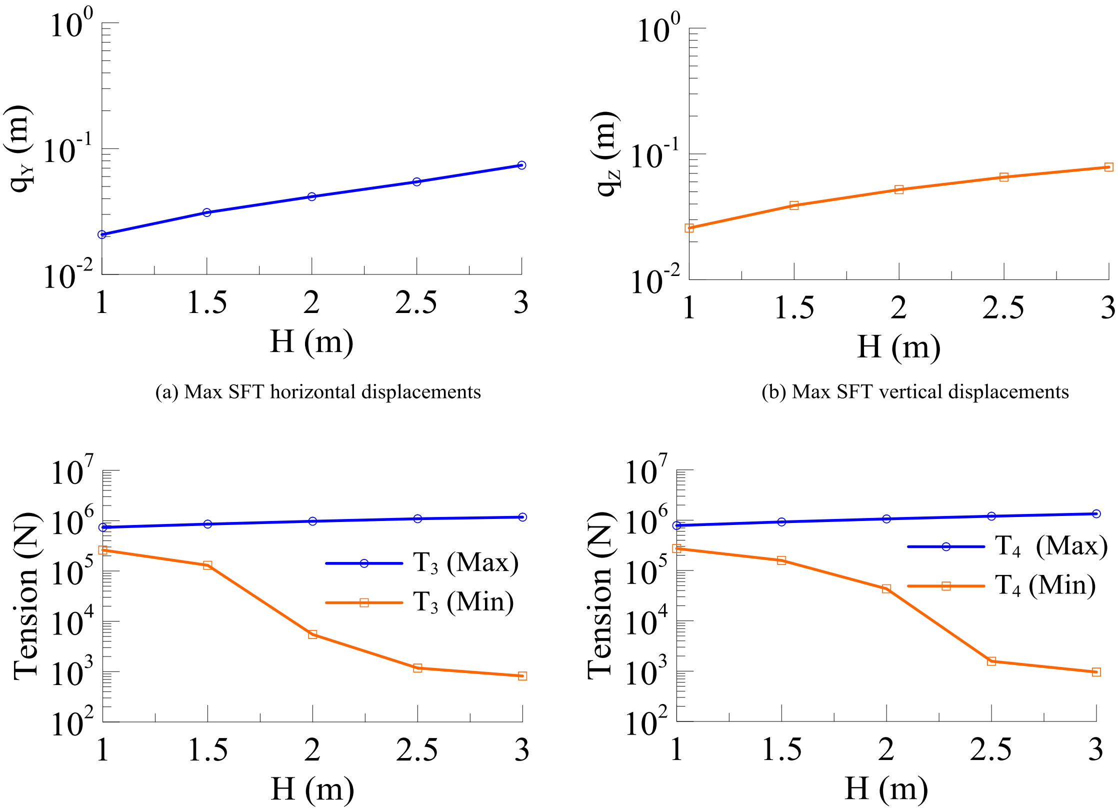

(a) Max SFT horizontal displacements

(b) Max SFT vertical displacements

(c) Max/Min cable top tension, T at C3

(d) Max/Min cable top tension, T at C4

Figure 4: Effect of wave height on maximum SFT displacements and maximum/minimum cable top tensions at location B under waves (T=2.3 s, ζ=2.5%)

CONCLUSION

The dynamic problem of SFT is formulated considering 3D tunnel and 3D cables. The tunnel is modeled by finite element method and cables are modeled by 3D catenary elements. The waves are modeled by Airy wave theory and wave forces are calculated by modified Morison's equation. The SFT behavior is evaluated under hydrodynamic and vertical ground motions. A comparison of SFT responses and cable top tensions is presented using truss and catenary cables. The following conclusions can be drawn from the numerical simulations performed:

(1) Wave forces are dominant actions for the analysis of SFT. The wave forces cause extreme tunnel displacements that can cause the mooring cables to become slack.

(2) The responses of SFT and cable top tensions show very similar trends using truss or catenary cables, however catenary cable gives slightly larger responses and therefore, could be very useful for very deep SFT having long cables.

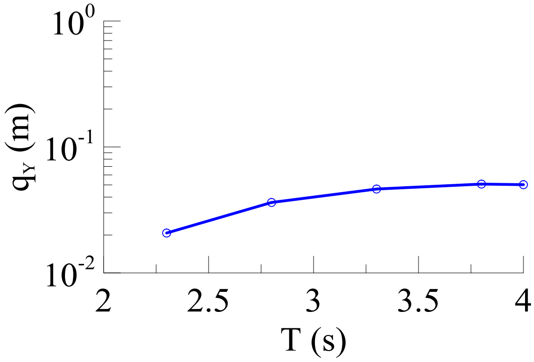

(a) Max SFT horizontal displacements

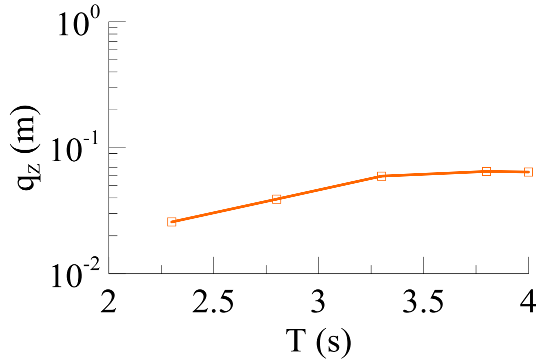

(b) Max SFT vertical displacements

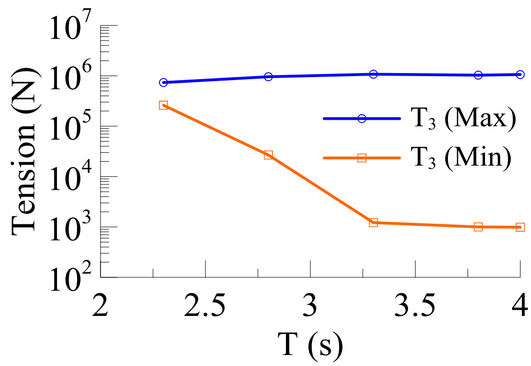

(c) Max/Min cable top tension, T at C3

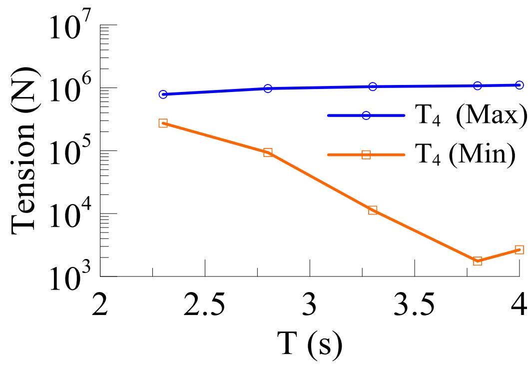

(d) Max/Min cable top tension, T at C4

Figure 5: Effect of wave period on the maximum SFT displacements and maximum/minimum cable top tensions at location B under waves (H=1 m, ζ=2.5%)

REFERENCES

- Ahrens D. (1997). Submerged floating tunnels a concept whose time has arrived. Tunnelling and Underground Space Technology 12(2): 317-336.
- Brancaleoni F, Castellani A, D'Asdia P. (1989). The response of submerged tunnels to their environment. Engineering Structures 11(1): 47-56.
- Chakrabarti S K. (1987). Hydrodynamics of offshore structures: WIT press. Offshore Structure Analysis Inc, USA.
- Di Pilato M, Feriani A, Perotti F. (2008). Numerical models for the dynamic response of submerged floating tunnels under seismic loading. Earthquake Engineering & Structural Dynamics 37(9): 1203-1222.
- Di Pilato M, Perotti F, Fogazzi P. (2008). 3D dynamic response of submerged floating tunnels under seismic and hydrodynamic excitation. Engineering Structures 30(1): 268-281.
- Faggiano B, Landolfo R, Mazzolani F. (2005). The SFT: an innovative solution for waterway strait crossings. International Association for Bridge and Structural Engineering. IABSE Symposium Report 90(10):36-42.

- Fogazzi P, Perotti F. (2000). The dynamic response of seabed anchored floating tunnels under seismic excitation. Earthquake Engineering & Structural Dynamics 29(3): 273-295.

- Li J, Li YS. (2006). Analytical solution to the vortex-excited vibration of tether in the submerged floating tunnel. In Underground Construction and Ground Movement. Pp. 164-169.

- Long X, Ge F, Hong Y. (2015). Feasibility study on buoyancy–weight ratios of a submerged floating tunnel prototype subjected to hydrodynamic loads. Acta Mechanica Sinica/Lixue Xuebao 31(5): 750-761.

- Long X, Ge F, Wang L, Hong Y. (2009). Effects of fundamental structure parameters on dynamic responses of submerged floating tunnel under hydrodynamic loads. Acta Mechanica Sinica 25(3): 335-344.

- Luoa G, Chen J, Zhou X. (2015). Effects of various factors on the viv-induced fatigue damage in the cable Of submerged floating tunnel. Polish Maritime Research 22(4): 76-83.

- Muhammad N. (2018). Dynamic Responses of Submerged Floating Tunnels with Mooring Cables under Waves, Earthquakes, and Moving Loads. Ph.D. Thesis, Hanyang University.

- Muhammad N, Ullah Z, Choi DH. (2017). Performance evaluation of submerged floating tunnel subjected to hydrodynamic and seismic excitations. Applied Sciences 7(11):1122.

- Muhammad N, Ullah Z, Choi DH. (2018). A numerical procedure accounting for fluid drag forces and cable extensibility for the static response of mooring cables. International Journal of Steel Structures 18(1): 293-303.

- Muhammad N, Ullah Z, Park MW, Choi DH. (2017). The role of cable stiffness in the dynamic behaviours of submerged floating tunnel. MATEC Web Conferences. The 6th International Conference of Euro Asia Civil Engineering Forum. 138:1-7.

- Okstad KM, Haukas T, Remseth S, Mathisen KM. (1998). Fluid-structure interaction simulation of submerged floating tunnels. Computational Mechanics. Barcelona, Spain. Pp. 1-13.

- Remseth S, Leira BJ, Okstad KM, Mathisen KM, Haukas T. (1999). Dynamic response and fluid/structure interaction of submerged floating tunnels. Computers & Structures 72(4–5): 659-685.

- Veritas DN. (2006). Free spanning pipelines. Recommended practice DNV-RPF105. Pp. 1-46.

- Yiqiang X, Chunfeng C. (2012). Vortex-induced dynamic response analysis for the submerged floating tunnel system under the effect of currents. Journal of Waterway, Port, Coastal, and Ocean Engineering 139(3):183-189.